2018 IEEE International Conference on Robotics and Automation (ICRA)
May 21-25, 2018, Brisbane, Australia

Exploration and Inspection with Vine-Inspired Continuum Robots

Michael Wooten[1], Chase Frazelle[1], Ian D. Walker[1], Apoorva Kapadia[1], and Jason H. Lee[2]

Abstract— **In this paper, we show how structures and strategies employed by thin-stemmed plants can be adapted to improve robot access to unstructured and congested environments. Specifically, we show how the use of vine-inspired movement strategies can enhance long thin continuum robot exploration and inspection operations. We introduce a new theoretical plant growth-inspired approach for modeling and motion generation of continuum robot backbones. The approach is demonstrated in numerous experiments including inspection within a high fidelity, full-scale mock-up of the International Space Station at NASA Johnson Space Center, using novel robot tendril hardware.**

I. Introduction

Biology has often been used as a source of inspiration in robotics [1], derived from natural arms, legs, tails, etc.. Perhaps the most recognizable instances of robots emulating nature are those made from discrete sets of joints serially-connected by rigid links, resembling the biological structure of vertebrate limbs with similar functions [2].

A more recent subset of the field is that of continuum robots, which is inspired by elephant trunks, octopus arms, and vines, an example of which is shown in Figure 1. These robots differ from traditional designs by incorporating a continuous backbone, rather than having discrete joints. Consequently, they are capable of bending along their entire length. This feature allows some continuum robots to reach spaces that traditional rigid-link robots cannot negotiate due to their inflexible structure. This is particularly true of thin continuum robots, defined here as those with backbone length several orders of magnitude greater than the diameter, which can access narrow, highly congested areas like dense undergrowth, densely packed equipment, and inside the human body [3] [4] [5].

Thin continuum robots are inherently compliant, and this feature serves them well in numerous medical procedures [5] in which they can gently navigate tubular environments which also provide structural support. However, in wider classes of applications featuring the need to cross voids as discussed herein, these robots face difficulties supporting their weight and and maintaining accuracy.

In order to address these issues researchers have recently been taking inspiration from plants [6], notably vines [7] [8] [9]. Related work is also inspired by plant roots [10] [11] [12]. Vines in particular need to combat the issue of crossing voids with thin structures and have developed numerous strategies to compensate for their lack of internal structural support. These methods often involve exploratory motion primitives supported by some form of environmental bracing. For example, many plants have adopted a method for growing called circumnutation. This pattern increases the likelihood that environmental support will be encountered [13].

In this paper we discuss and demonstrate how some of these botanical strategies can be exploited and adapted to thin continuum robots exploring and inspecting congested environments while crossing voids. Based on a theoretical model used to analyze plant growth [14], we introduce new techniques for modeling and motion-primitive generation, including circumnutation, for continuum robots. The analysis is supported by experiments using novel long thin vine-inspired continuum robot hardware, including inspection in a high fidelity International Space Station module at NASA Johnson Space Center.

The paper is organized as follows. In the following section, we discuss relevant plant behaviors and introduce the theoretical model and associated new algorithms underlying this work. Section III describes the vine-inspired robot used for hardware implementation of the algorithms. Simulations and laboratory experiments are reported in Section IV, with field experiments and the Space Station environment demonstration discussed in Section V. Conclusions are presented in Section VI.

Fig. 1: Three section, spring-loaded concentric tube continuum robot with three tendons per section allowing local backbone extension and bending in all directions.

*This work is supported in part by the U.S. National Science Foundation under grant IIS-1527165, and in part by NASA under contract NNX12AM01G

[1]Michael Wooten, Chase Frazelle, Ian Walker, and Apoorva Kapadia are with the Department of Electrical and Computer Engineering, Clemson University, Clemson, SC 29634, USA mbwoote,cfrazel,iwalker,akapadi@clemson.edu

[2]Jason Lee is with the Robotic Systems Technology (ER4) Branch, NASA Johnson Space Center, Houston, TX, USA Jason.Lee@nasa.gov

II. Plant-Inspired Innovations

In a long thin vine-like tendril robot, its profile results in a lack of structural support, often leading to sagging and buckling, and the issue of how best to move within unexplored environments remains unresolved. Plants, and in particular vines, face similar issues. However, their biological capabilities have evolved to include the means to successfully overcome these problems, notably by actively engaging the environment to increase stability. Notice that this is counter to the usual mode of robot navigation, wherein environmental contact is generally avoided when possible.

Plants also use motion primitives, commonly circumnutation, when growing into an environment to enhance the probability of encountering such support. Collectively, these features allow the plants to expend energy towards linear, rather than axial, growth [15] [16]. Though a locally extensible version of the robot discussed in this paper was developed [7], the robot used for the following experiments was not designed with the capability to mimic a plant's ability to grow into an environment. Instead the focus of this paper was to adopt physical plants' movement strategies.

A. Plant-Inspired Open Space Movement

Circumnutation is the elliptical pattern of movement displayed by the tips of many plants (and some roots [12]) as they grow. These oscillations during growth increase the plant's opportunity for finding and exploiting structural support in the environment [17]. The growth and exploration aspects of plant physics [18] as well as the circumnutation movement [19] have been studied in detail. The issue of how to move tendril-like robots to explore *a priori* unknown environments remains open. Circumnutation provides an "existence proof" from nature, which is noted to be both energy-efficient and optimal for plants.

Circumnutation could have high potential to improve robot tendril performance if incorporated into the design and operation of a tendril robot [20], rendering it similarly capable of efficiently making contact with and subsequently using the environment for support.

B. Theory of Circumnutation

To describe plant-like motion, an analytical form suitable for implementation by continuum robots, and to conveniently generate circumnutation-like motion profiles, we introduce herein a new kinematic model for continuum robots based on differential growth. The model is adapted from the computational biology [14], in which a kinematic model for interpretation of circumnutation patterns observed in plants was recently proposed. The key underlying concept is to relate, for a given section, changes in its curvature $k(t) \in \Re$ and orientation $\phi(t) \in \Re$ to longitudinal length changes along its perimeter.

For simplicity, we assume that the circumnutation is created using a single section (the most distal), and that the section assumes constant curvature along this section at any given instant of time (but that the value of k is time varying). The initial length along the center line of the section is given as L_0, and the radius of the section, assumed to be constant, is R. The initial curvature of the section is $k(0)$, and its initial orientation of maximum curvature, with respect to a coordinate frame fixed at its base and with its $z-$axis aligned with the section tangent there, is $\phi(0)$.

Given these assumptions, the length $L_s(\theta)$ of a line along the outside of the section, parallel to the center line, and at a constant angle θ with respect to ϕ, as measured in the plane orthogonal to the section tangent, is given by:

$$L_s(\theta) = L_0(1 - Rkcos(\theta - \phi)) \tag{1}$$

We next consider a deformation of the section, resulting in a new center line length of L_0^1, new curvature $k^1(t)$, and new orientation of maximum curvature $\phi^1(t)$. We have, at orientation θ about the exterior,

$$L_s^1(\theta) = L_0^1(1 - Rk^1cos(\theta - \phi^1)) \tag{2}$$

The elongation strain $\epsilon(\theta)$ at a given orientation θ around the section exterior is defined to be the ratio between the elongation length $[L_s^1(\theta) - L_s(\theta)]$ and the original length $L_s(\theta)$:

$$\epsilon(\theta) = [L_s^1(\theta) - L_s(\theta)]/L_s(\theta) = [L_s^1(\theta)/L_s(\theta)] - 1 \tag{3}$$

For a continuum section actuated by three tendons arranged at 120^o intervals as for the tendril in this paper, the average elongation strain rate E is given by:

$$E = (1/3)\Sigma_{i=1}^{3}(\epsilon_i) \tag{4}$$

where ϵ_i is the strain at the orientation of the i^{th} tendon. Then, the deformed center line $L_0^1 = L_0(1+E)$, and equation (2) becomes

$$L_s^1(\theta) = (1 + E)L_0(1 - Rk^1cos(\theta - \phi^1)) \tag{5}$$

Combining (1), (3), and (5) results in

$$\epsilon(\theta) = (1 + E)\frac{(1 - Rk^1cos(\theta - \phi^1))}{(1 - Rkcos(\theta - \phi))} - 1 \tag{6}$$

By introducing an infinitesimal time step and deformations $\epsilon(\theta) = \dot{\epsilon}(\theta)dt$, $E = \dot{E}dt$, $k^1 = k + dk$, and $\phi^1 = \phi + d\phi$, and then expanding the above expression (and neglecting terms of second order infinitesimals), we obtain a differential equation describing the underlying kinematics as:

$$\dot{\epsilon}(\theta) = \dot{E} + \frac{kRsin(\theta - \phi)\dot{\phi} + Rcos(\theta - \phi)\dot{k}}{(1 - Rkcos(\theta - \phi))} \tag{7}$$

This expression provides the rate of change of exterior fiber length, at orientation θ radially about the section, corresponding to a given rate of change of configuration $(\dot{k}, \dot{\phi})$ and average elongation rate $\dot{E}$. In [14], the authors use the above model to analyze the observed growth and circumnutation behavior in plants. They note that, defining differential growth Δ as the difference between elongation

strain rates on opposite sides of the structure, divided by the average strain rate,

$$\Delta(\theta, t) = \frac{\dot{\epsilon}(\theta, t) - \dot{\epsilon}(\theta + \pi, t)}{2\dot{E}(t)} \tag{8}$$

when expanding the expressions for $\Delta(\phi, t)$ and $\Delta(\phi + \pi/2)$, the model in (7) simplifies to

$$\dot{k} = \Delta(\phi, t)\dot{E} \tag{9}$$

and

$$\dot{\phi} = [\Delta(\phi + \pi/2)\dot{E}]/Rk \tag{10}$$

respectively. (In the first of these expressions, the small quadratic terms are neglected.)

Equations (9) and (10) provide an intuitive model showing how section configuration shape rates $(\dot{k}, \dot{\phi})$ can be generated from differential growth (Δ) and average elongation rate $\dot{E}$. Note that $\Delta(\phi)$ is the difference in growth rates on opposite sides of the section in the plane of maximum curvature, producing in-plane changes in curvature, and $\Delta(\phi + \pi/2)$ is the equivalent growth rate difference in the plane orthogonal to this, producing out-of-plane changes in section orientation. The configuration rate changes are in each case also linearly related to the average elongation strain rate $\dot{E}$.

The authors of [14] use the model to postulate possible growth rates underlying observed circumnutation data in natural plants. In this paper however, we adapt the model to the problem of modeling and generating circumnutation movements in tendon-driven continuum robots. In this situation, we cannot assume the ability of the structure to grow at arbitrary locations of θ about the structure, as with biological plants. Note again that, for the tendril robot in this paper and numerous other tendon-driven continuum robots, there are three tendon actuators per section, spaced at 120^o apart in $\theta-$space. Methods of analyzing and generating motions, including circumnutations, in such continuum robots need to take this into account.

To do this, we note that in [14] the differential growth rates can be found as projections of a (as yet unknown) direction θ_g of maximal principal growth $\Delta(\theta_g)$:

$$\begin{aligned} \Delta(\phi) &= \Delta(\theta_g)cos(\theta_g - \phi) \\ \Delta(\phi + \pi/2) &= \Delta(\theta_g)sin(\theta_g - \phi) \end{aligned} \tag{11}$$

If the direction θ_g of maximal principal growth is aligned with one of the three actuators in a continuum robot, and the direction is fixed at this angle, then it can be found, using (9) - (11), that the orientation ϕ of the plane of maximum curvature is driven to align with the direction θ_g of maximum growth, and (using (11)) will remain there. In other words, driving the section with a dominant, single actuator (θ_g will thus become the radial angle corresponding to its tension) will rotate it to align the direction of maximum curvature with that actuator, a result which makes intuitive sense. This observation suggests a new approach to the modeling and generation of continuum robot circumnutations: the elongation of tendons in sequence (note that the tendril is spring loaded, so tendon tension can decrease), successively cycling from tendons i to $i + 1$, and switching when the plane of curvature matches the tendon location. This strategy directly provides both the rotation and extension motions underlying circumnutation.

The above observations and resulting approach to motion primitive generation (Section IV) is completely new to the best of our knowledge, and proves to be effective in generating circumnutations in continuum tendril robots. In subsequent sections, we describe thin-continuum tendril robot hardware (Section III) configured to take advantage of new circumnutation motion primitives (Section IV). Next, however, we discuss a second thin plant-inspired strategy, that of environmental contact.

C. Plant-inspired Environmental Contact

Many vines help support their highly compliant structures by seeking out and leveraging fixed environmental support via permanent contacts, using specialized structures emerging from their backbones (prickles, roots or pad structures) [15]. Mimicking this strategy, the concept of using primitive artificial prickles (Figure 2) was developed previously [7]. It was found that actively engaging the environment reduced, and in most cases eliminated, coupling proximal to the point of contact [7].

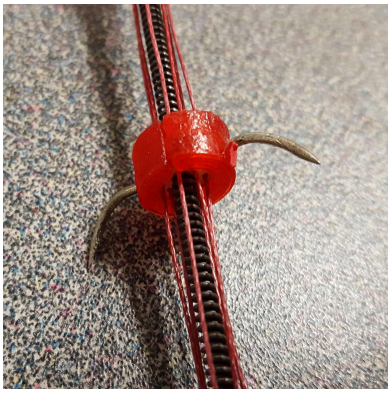

Fig. 2: Example of artificial prickle installed on tendril robot backbone.

This prickle design was proved to be effective in a few cases [7], but in some cases difficult to utilize in exploration experiments. Environmental interaction required precise orientation to engage the environment reliably. The prickles also required a suitable type of attachment point, which had a sufficiently small diameter such that the prickle could fit around the environmental feature. Furthermore, the prickles could pierce and sink into an attachment point and become stuck in place, making detaching difficult.

Additionally, specialized hardware for solid robot attachment to the environment increases mechanical complexity, and increases the profile of the backbone, reducing its ability to maneuver through tight spaces. Consequently, an alternative and simpler approach to environmental contact

exploitation for tendril robots, which does not involve modifications to their basic structure, is suggested herein.

Some plants and vines exploit non-permanent contacts with the environment without use of specialized contact structures, essentially bracing against stable environmental features with their stems to gain mechanical advantage. The idea of bracing for conventional robots has been considered previously [21] [22] [23]. However, the concept does not appear to have been formally considered for continuum robots. In Sections IV and V, we demonstrate the advantage and inherent simplicity of implementations using this approach with tendril-like robots.

In the following section, novel robot hardware suitable for the implementation of the theory and operational concepts introduced in this section is described.

III. Plant-Inspired Continuum Robot Hardware

The underlying design for the continuum robot considered herein is based on a spring-loaded concentric tube backbone that is entirely actuated by tendons [7]. The backbone core consists of three concentric, telescopic, carbon fiber tube sections. The middle and tip sections are spring loaded allowing for local extension and contraction. These springs are separated by 3D-printed plastic spacers, equipped with at least nine outer holes through which tendons are routed to facilitate actuation. There are three such tendons terminated at the tip of each section, allowing two tendon-actuated degrees-of-freedom bending per tube. The section lengths were selected to be 21.9, 34.6, and 89.4 cm for the tip, middle, and base sections respectively with a maximum spacer diameter of 1.6 cm.

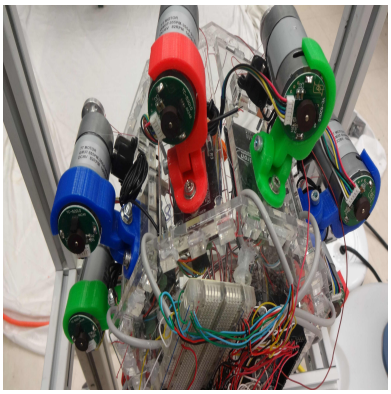

Fig. 3: Tendril robot actuator package featuring nine DC motors all resting on load cells for tension sensing.

The actuator package comprises nine DC motors concentric to the robot backbone. Each motor feature encoder feedback, allowing for direct feedback control. The motors are operated using an Arduino Due via a motor driver, which allows for speed control using a PWM signal.

Each of the motors rests on a load cell, allowing for measurement of approximate tension feedback. The combination of encoder feedback and tension sensing allows for a more accurate estimation of tendon length than previous designs, to determine robot shape [24].

For the NASA demonstration reported in Section V, the actuator assembly was mounted in a frame which provided two additional degrees of freedom: one active, a vertical hoist actuated by a single DC motor, and one passive, a manually operated rotational pitch which was locked in place after an initial pitch angle was selected, as seen in Figure 4.

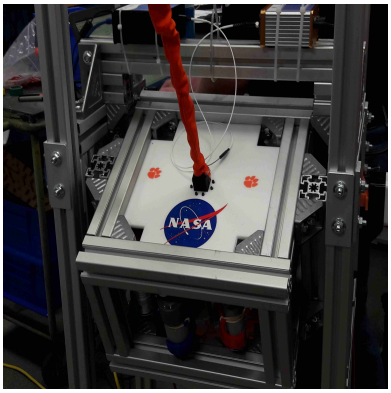

Fig. 4: Frame containing actuator package featuring active height control and lockable pitch adjustment mechanism.

IV. Simulations and Lab Experiments

The kinematic model from Section II was integrated into the simulation and real-time tendril control software environment in our laboratory. MATLAB [25] in order to model tendril sections in 3D space. The model operates by plotting incremental points along the backbone of the tendril based on the kinematic model in Section II-B. These points are plotted in cartesian coordinates using the 3D plotting package built into MATLAB.

In order to implement circumnutation motion primitives with the tendril robot, the tendons needed to be actuated in sequence. Such sequencing was achieved using a pattern of changing encoder counts. A small example portion is given in Table I. Each row in the table represents a set of encoder counts sent to the robot at once. Every time this occurs, the robot moves each motor for which the target encoder counts changes, i.e. implementing in hardware, the theory of circumnutation in Section II-B. This particular sequence of counts gives rotation and extension thus the appearance of growing, much like a plant would.

The circumnutation motion primitives are programmed algorithmically, which is a formalization of the *ad hoc* approach in [20] to allow the movement to be made with any given section, or multiple sections. Consequently, before beginning the movement a user must first choose any combination of sections to perform the circumnutation movements. After the choice is made each set of motors that need to move are loaded into the circumnutation function in the control code. These motor numbers include 0-2 for the base section, 3-5 for the middle, and 6-8 for the tip. Therefore, if choosing the tip and middle section, the array [3, 4, 5, 6, 7, 8] would be sent as input to the circumnutation function. This function would then wind both motors 3 and 6, record their respective

Motor 1 Encoder	Motor 2 Encoder	Motor 3 Encoder
5000	5000	5000
4800	5000	5000
4800	4600	5000
4800	4600	4400
4200	4600	4400
4200	4000	4400
4200	4000	3800
3600	4000	3800

TABLE I: Example encoder count sequence that results in circumnutation movement.

tensions and next wind motors 4 and 7 to that tension. This pattern repeats, looping back to the first motors at the end of the sequence, until a predefined maximum number of iterations is achieved. This procedure results in a motion primitive that very closely mimics the circumnutation of a vine as it grows.

An example simulation is shown in Figures 5 and 6. Stop motion plotting of circumnutation is captured by plotting several instances of motion on a single set of axes. Figure 5 shows a sequence of points along a single rotation of the distal section. Figure 6 demonstrates the growth of the distal section over a series of rotations.

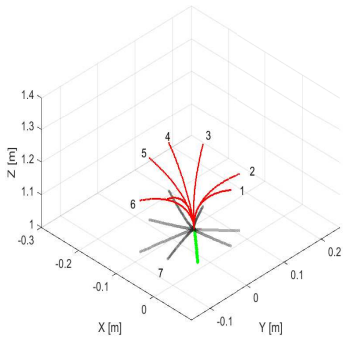

Fig. 5: Time lapsed circumnutation simulation with numbered frames.

A sequence of images illustrating the implementation of

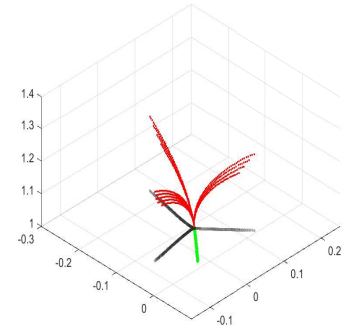

Fig. 6: Simulation of circumnutation motion.

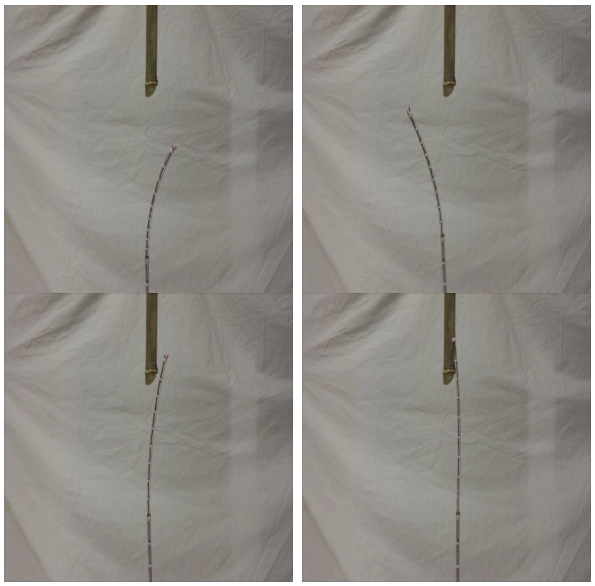

Fig. 7: Circumnutation with tendril robot.

the circumnutation motion primitive in the robot hardware is shown in Figure 7 and the video accompanying this paper. These motions were produced in the hardware using the encoder count values in Table I.

Additionally, we evaluated alternative strategies for passive bracing of the backbone. The bracing configuration adopted in one such experiment is shown is Figure 8. Here the tendril robot is depicted entering a water cooler jug and bending to look back on itself. As the robot enters further into the jug, the backbone braces against the end of the jug, allowing for bending in the tip previously unobtainable. This demonstrated some of the benefits to simple bracing.

Fig. 8: Robot tendril backbone braced against environment. Top-left: Jug, Top-right: Tendril entering jug, Bottom-left: max unbraced bending, Bottom-right: Bending with bracing.

V. Field Testing and Space Station Demonstration

A. Inspection of Congested, Outdoor Environments

The tendril robot was deployed in a variety of outdoor natural environments. The main goal was to determine what settings and environments the tendril robot performed best in, and to identify what operational difficulties it faced.

The robot was configured with a tip camera, to validate and document its ability to reach and inspect remote environments. At each site, previously unknown to the team, the goal was to evaluate the tendril robot in scenarios that demonstrated a combination of abilities unique to thin continuum robots. The experimental criteria were as follows:

1) Spanning a void.
2) Navigating highly congested areas.
3) Inspecting enclosed areas.
4) Maintaining a consistent presence.

The locations and tasks selected each complied with at least two of the aforementioned experiment criteria. Other technologies, including robotic vehicles and drones, may be capable of performing similar tasks satisfying one or two of the aforementioned criteria. However, the tendril robot described here is capable of performing all four. The experiments showcase the ability of tendril robots to do so.

1) Spanning Stream Into Storm Drain: For this experiment the tendril robot was deployed across a small stream in order to search a storm drain for signs of life. To avoid the water, the robot had to demonstrate the ability to span the void over the stream that was approximately 0.75 meters wide. Next, it had to turn into a semi-enclosed space and observe earthworms inside the drain, shown in Figure 9.

Fig. 9: Spanning stream and searching a storm drain for signs of life. Top to bottom, left to right: increasing time.

2) Inspecting Inside a Dead Tree: The tendril robot was used to inspect the inside of a dead tree stump, shown in Figure 10, through a knot-hole that was approximately three centimeters in diameter. This location was chosen specifically because of the small diameter hole the tendril robot had to pass through to inspect the interior. Once inside, the robot was able to cross the void below the opening and inspect the outside the stump via two holes on either side, as well as the floor of the stump. In doing this, the tendril robot passed through a highly congested area, crossed a void, and inspected a partially enclosed area.

Fig. 10: Inspecting a dead tree through small knot hole. Top to bottom, left to right: increasing time.

3) Investigating a Natural Cave in River Bank: In Figure 11 the tendril is depicted moving downwards through heavy underbrush, demonstrating the ability to navigate a highly congested area. The undergrowth is at the top of a river bank, with the entrance of a cave-like animal habitat below it. As the robot is lowered beyond the undergrowth, it also is moving across a void. In the last image, the robot turns to look inside the enclosed area.

Fig. 11: Investigating side of a river bank. Top to bottom, left to right: increasing time.

Collectively, these experiments demonstrated the ability of the robot, using circumnutation-like movements, to explore congested environments, crossing voids where necessary.

B. Space Station Inspection Demonstration

We further illustrate the potential of plant-inspired tendril robots via a demonstration of remote inspection within the Payload Development Laboratory II (PDLII) - a full scale, high fidelity module mock-up of the International Space Station (ISS). NASA has operational needs motivating the

development of tendril-like robots [26], in particular for inspections within and behind the equipment and life support racks in the ISS [7]. The capabilities of the tendril robot were demonstrated and evaluated by NASA within PDLII, which contains high fidelity examples of such racks.

The robot is shown within the mock-up environment at the NASA Johnson Space Center in Houston in Figure 12. The demonstration was conducted in June 2017.

Fig. 12: Robot in Space Station mock-up environment. Tendril backbone has orange covering.

To access and inspect within each rack, it was necessary to pass through nested layers of equipment, such as fragile wire bundles and piping, and in one case a flexible webbing, as seen in Figure 13.

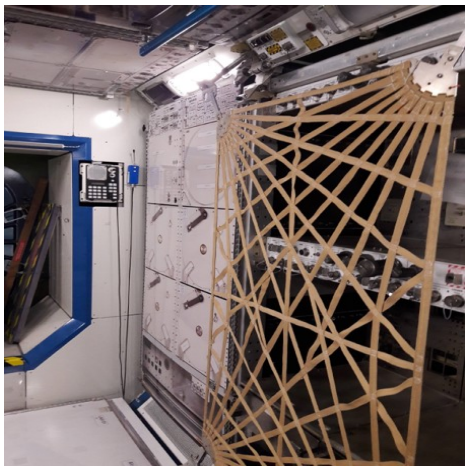

Fig. 13: View of one of the racks to be inspected.

To inspect between and behind the racks, a deep (27 to 38 inch) but narrow (less than 1 inch gap) void between the racks had to be negotiated, as seen in Figure 14, followed by a sharp 90 degree turn to access the back wall. To negotiate the turn, the robot successfully utilized passive bracing as discussed in Section II, bracing against the mounting bracket at the rear end of the rack.

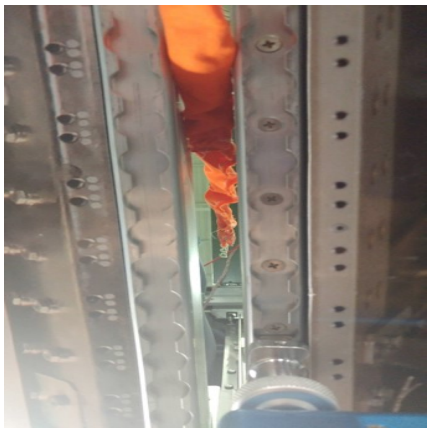

Fig. 14: Tendril robot penetrating gap between two racks.

The robot was able to successfully penetrate the space between the racks, reaching and accessing the back wall of the module. Images captured during these experiments included views of the frame at the rear, between racks, (top-left of Figure 15) and a physical anomaly on the rear wall of the module (top-right Figure 15). The ability to access and view such anomalies has strong operational significance, as there is a need to inspect for micrometeorite damage to the external walls of the Space Station in addition to inspecting sensitive and nearly inaccessible operating equipment.

The robot was also able to successfully penetrate, navigate within, and return detailed images of the condition of structures (Figure 15 bottom), and of cables and their labeling (Figure 16) within and behind the equipment in the racks.

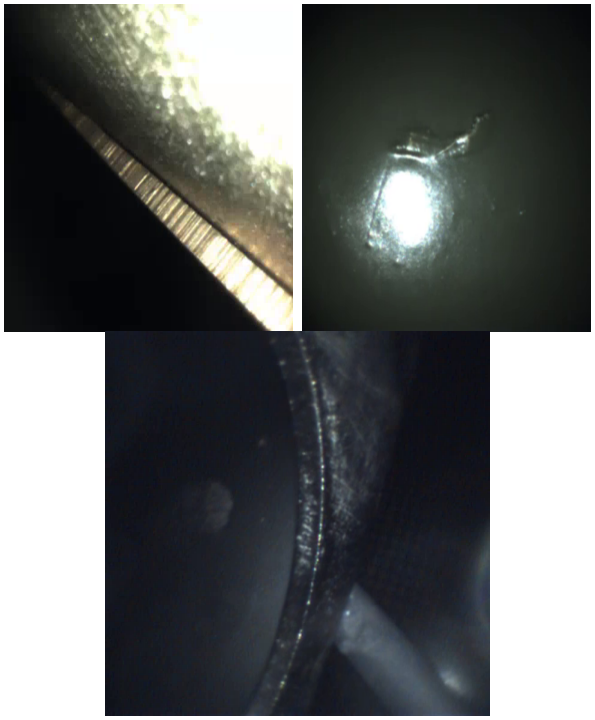

Fig. 15: Images of structure within racks and behind equipment.

Fig. 16: Labeling behind equipment within rack and a close up view.

These operations, providing images and information previously unobtainable without the laborious and crew member time-intensive procedure of removing individual racks and the equipment within them, establish a new and highly useful robotic inspection option for NASA. The addition of a simple end effector could expand this option to include manipulation. The crew currently spends significant time routing cables through the ISS. If the tendril could attach to and route cables throughout the station, this could save time and effort, and provide NASA a useful new resource. Our current efforts focus on refining the hardware suitable for a flight experiment on the ISS. Overall, the demonstrations reported herein illustrate both the unique capabilities of long thin continuum robots in performing remote inspection operations, and the advantages of employing plant-inspired strategies in doing so.

VI. CONCLUSIONS

We have discussed the advantages and inherent physical limitations of long thin continuum robots in inspection operations. Various ways in which thin plants, notably vines, overcome these limitations were reviewed and discussed. Based on a new kinematic model introduced herein, we have proposed a new approach to generating basic movements, considered optimal in plants, for tendril-like robots, to explore and actively contact their environment. Unique capabilities achievable using this vine-inspired approach are demonstrated using a three section tendril robot, in laboratory and outdoor testing, as well as via an inspection demonstration in a NASA Space Station mock-up. At the submission of this paper, the full impact of environmental contact is still not understood, and a comprehensive comparison between experimental and simulated results has not been completed.

REFERENCES

[1] D. Trivedi, C. Rahn, W. Kier, and I. Walker, "Soft robotics: Biological inspiration, state of the art, and future research," *Applied Bionics and Biomechanics*, vol. 5, no. 3, pp. 99–117, September 2008.

[2] J.-A. Meyer and A. Guillot, *Biologically Inspired Robots*, ch. 60, pp. 1395–1418.

[3] I. Walker, "Continuous backbone "continuum" robot manipulators: A review," *ISRN Robotics*, vol. 2013, no. 1, pp. 1–19, July 2013.

[4] G.Robinson and J. Davies, "Continuum robots - a state of the art," in *Proceedings IEEE International Conference on Robotics and Automation*, Detroit, Michigan, 1999, pp. 2849–2854.

[5] J. Burgner-Kars, D. Rucker, and H. Choset, "Continuum robots for medical applications: A survey," *IEEE Transactions on Robotics*, vol. 31, no. 6, pp. 1261–1280.

[6] P. Martone, M. Boller, I. Burgert, J. Dumais, J. Edwards, K. Mach, N. Rowe, M. Rueggeberg, R. Seidel, and T. Speck, "Mechanics without muscle: Biomechanical inspiration from the plant world," *Integrative and Comparative Biology*, vol. 50, no. 5, pp. 888–907.

[7] M. Wooten and I. Walker, "A novel vine-like robot for in-orbit inspection," in *Proceedings 45th International Conference on Environmental Systems*, Bellevue, Washington, 2015, pp. 1–11.

[8] E. Hawkes, L. Blumenschein, J. Greer, and A. Okamura, "A soft robot that navigates its environment through growth," in *Science Robotics*, 2017.

[9] L. H. Blumenschein, A. M. Okamura, and E. W. Hawkes, "Modeling of bioinspired apical extension in a soft robot," in *Living Machines*, 2016.

[10] B. Mazzolai, L. Beccai, and V. Mattoli, "Plants as model in biomimetics and biorobotics: New perspectives," *Frontiers in Bioengineering and Biotechnology*, vol. 2, pp. 1–5.

[11] A. Sadeghi, A. Tonazzini, I. Popova, and B. Mazzolai, "Robotic mechanism for soil penetration inspired by plant root," in *Proceedings IEEE International Conference on Robotics and Automation*, Karlsruhe, Germany, 2013, pp. 3457–3462.

[12] E. D. Dottore, A. Mondini, A. Sadeghi, V. Mattoli, and B. Mazzolai, "Circumnutations as a penetration strategy in a plant-root-inspired robot," in *Proceedings IEEE International Conference on Robotics and Automation*, May 2016, pp. 4722–4728.

[13] C. Darwin, *The Movements and Habits of Climbing Plants*. John Murray.

[14] R. Bastien and Y. Meroz, "The kinematics of plant nutation reveals a simple relation between curvature and the orientation of differential growth," *PLOS Computational Biology*, vol. 12, no. 12.

[15] A. Goriely and S. Neukirch, "Mechanics of climbing and attachment in twining plants," *Physical Review Letters*, vol. 97, no. 18, pp. 1–4.

[16] F. Putz and H. Mooney, *The Biology of Vines*. Cambridge University Press.

[17] S. Isnard and W. Silk, "Moving with climbing plants from charles Darwin's time into the 21st century," *American Journal of Botany*, vol. 96, no. 7, pp. 1205–1221.

[18] A. Brown, "Circumnutations: From Darwin to space flights," *Plant Physiology*, vol. 101, pp. 345–348.

[19] K. J. Niklas and H.-C. Spatz, *Plant Physics*. University of Chicago Press.

[20] M. B. Wooten and I. D. Walker, *Circumnutation: From Plants to Robots*. Cham: Springer International Publishing, 2016, pp. 1–11.

[21] W. Book, S. Le, and V. Sangveraphunsiri, "The bracing strategy for robot operation," in *Proceedings 5th Symposium on Theory and Practise of Robots and Manipulators*, Udine, Italy, 1984, pp. 1–8.

[22] I. Bullock, R. Ma, and A. Dollar, "A hand-centric classification of human and robot dexterous manipulation," *IEEE Transactions on Haptics*, vol. 6, no. 2, pp. 129–144, April-June 2013.

[23] R. Hollis and R. Hammer, "Real and virtual coarse-fine robot bracing strategies for precision assembly," in *Proceedings IEEE International Conference on Robotics and Automation*, Nice, 1992, pp. 767–774.

[24] M. Tonapi, I. Godage, A. Vijaykumar, and I. Walker, "Spatial kinematic modeling of a long and thin continuum robotic cable," in *Proceedings IEEE International Conference on Robotics and Automation*, editor, Ed., Seattle, WA, pp. 3755–3761.

[25] MathWorks. (2017) Matlab. [Online]. Available: https://www.mathworks.com/products/matlab.html

[26] J. Mehling, M. Diftler, M. Chu, and M. Valvo, "A minimally invasive tendril robot for in-space inspection," in *Proceedings International Conference on BioRobotics*, Pisa, Italy, 2006, pp. 690–695.